JOURNAL OF AGRICULTURAL AND FOOD CHEMISTRY
ARTICLE

J. Agric. Food Chem. 2009, 57, 8459–8466 8459
DOI:10.1021/jf901571g

Metabolomic Change Precedes Apple Superficial Scald Symptoms

David R. Rudell,*,† James P. Mattheis,† and Maarten L.A.T.M. Hertog‡

†Tree Fruit Research Laboratory, USDA-ARS, Wenatchee, Washington 98801, and ‡BIOSYST-MeBioS, Katholieke Universiteit Leuven, Heverlee, Belgium

Untargeted metabolic profiling was employed to characterize metabolomic changes associated with 'Granny Smith' apple superficial scald development following 1-MCP or DPA treatment. Partial least-squares discriminant analyses were used to link metabolites with scald, postharvest treatments, and storage duration. Models revealed metabolomic differentiation between untreated controls and fruit treated with DPA or 1-MCP within 1 week following storage initiation. Metabolic divergence between controls and DPA-treated fruit after 4 weeks of storage preceded scald symptom development by 2 months. α-Farnesene oxidation products with known associations to scald, including conjugated trienols, 6-methyl-5-hepten-2-one, and 6-methyl-5-hepten-2-ol, were associated with presymptomatic as well as scalded control fruit. Likewise, a large group of putative triterpenoids with mass spectral features similar to those of ursolic acid and β-sitosterol were associated with control fruit and scald. Results demonstrate that extensive metabolomic changes associated with scald precede actual symptom development.

KEYWORDS: Metabolome; metabolic profiling; storage; diphenylamine; 1-methylcyclopropene

INTRODUCTION

Apples (*Malus sylvestris* L. (Mill.) var. domestica Borkh. Mansf.) are typically stored at −1 to 4 °C without any immediate injury (*1*); however, browning disorders that have been attributed to chilling stress at low storage temperatures can appear within weeks or months. These include superficial scald (scald) (*2*), a superficial peel necrosis that affects the first five or six hypodermal layers (*3*) and typically develops after ≥2 months of cold storage (*4*). Scald incidence can be reduced using prestorage or intermittent warming treatments (*2*, *5*).

Key defining features of scald incidence and development lie in the methods used to reduce or eliminate its incidence. Given the effectiveness of the antioxidants diphenylamine (DPA) (*6*) and ethoxyquin (*7*), it is likely that scald results from oxidative stress (*8*). Oxidation of α-farnesene in peel tissues is thought to play a key role in scald development on the basis of a range of findings. α-Farnesene levels increase with apple ripening in many scald-susceptible as well as scald-resistant cultivars (*9*−*11*). Conjugated trienols (CT) and 6-methyl-5-hepten-2-one (MHO) levels, both oxidized products of α-farnesene, can increase coincidently with scald (*9*, *12*, *13*), although not in all instances, especially when multiple cultivars or breeding selections are compared (*11*). DPA treatment prevents α-farnesene oxidation (*13*, *14*), whereas ethylene action (*15*, *16*) inhibitors, such as 1-methylcyclopropene (1-MCP), prevent or delay scald development, possibly by reducing α-farnesene biosynthesis (*15*). Catalytic activity of enzymes involved in reactive oxygen species generation or oxidative stress suppression is associated with the onset of chilling in apples (*17*, *18*), although no consistent correlation with scald is clear (*8*). Similarly, 1-MCP purportedly reduces oxidative stress-related enzyme activity in some instances (*19*).

Another key difference between scald and other chilling or freezing-related apple injuries is the relatively extended time period between cold storage initiation and superficial scald symptom development compared with other browning disorders. Scald inception occurs within the first 6−8 weeks of cold storage, during and after which scald control measures, including DPA and 1-MCP (*20*), become less effective (*4*). The actual physiological or metabolic events leading to scald during this induction period remain obscure.

α-Farnesene synthesis begins near harvest and is amplified by cold storage imposition, whereas CT formation occurs several weeks later (*10*, *12*). The buildup of CTs in the wax layers has been directly linked to tissue necrosis. Application of certain CTs onto intact apples provokes symptom development very similar to scald (*21*). Because CT levels in peel of cultivars with different susceptibilities to scald do not always correlate well with scald incidence, it is likely other factors also influence scald development (*11*). One prevailing theory bases these differences, at least in part, on variation of constitutive antioxidants from across sampling locations on peel from the same fruit or among different cultivars (*22*−*25*).

To date, scald research has been largely limited to the study of α-farnesene and antioxidant metabolism. Improvements in instrumentation and data analysis techniques are allowing more

*Author to whom correspondence should be addressed [telephone (509) 664-2280; fax (509) 664-2287; e-mail David.Rudell@ars.usda.gov].

Published on Web 08/28/2009

comprehensive study of plant metabolism using metabolomic approaches (*26*, *27*). Already, these tools have been applied to study commercially significant phenomena in important fruit crops including tomato (*28*−*30*), strawberry (*31*), pear (*32*), and apple (*25*, *33*).

To link apple peel metabolism to storage and scald during all stages of scald development, antioxidant and ethylene relationships were evaluated using profiling of peel primary and secondary metabolism during 6 months of cold storage. It was expected that cold storage inception and scald development would be characterized by extensive metabolic changes in multiple pathways.

MATERIALS AND METHODS

'Granny Smith' apples were harvested 140 days after full bloom (approximately 1 month prior to commercial harvest) at a research orchard near Orondo, WA. After transport to the laboratory, analysis of fruit maturity and application of DPA and 1-MCP were as previously described (*34*). Apples were stored in air at 1 °C for up to 6 months. Six replications of three fruits per treatment were removed from storage at 1, 2, and 4 weeks and 2, 3, 4, and 6 months. Upon removal from storage, scald development was rated on a 0−4 scale (*25*) and peel sampled and stored from each treatment for subsequent analysis. In a parallel experiment, additional apples were treated with 2000 mg L^{-1} DPA after 1−4 weeks and 2 months after storage inception to determine the length of the transitional period during which scald can be suppressed. Scald development on these fruits was evaluated after 2, 3, 4, and 6 months of storage.

Tissue Processing and Trimethylsilyl(oxime) Derivative Analysis. Frozen peel was cryogenically milled to a fine powder and stored at −80 °C prior to metabolite analysis. Frozen peel powder was analyzed using three extraction procedures and four instrumental analyses to evaluate the metabolome. Methanolic extraction coupled with trimethylsilyl(oxime) derivatization and GC-MS analysis of frozen apple peel powder was as described previously (*33*).

Volatile Metabolite Analysis. Frozen peel powder (0.5 g) was weighed into 20 mL glass headspace vials (Gerstel, Baltimore, MD) previously chilled in N_2 (l). Vials containing sample were removed from N_2 (l), 1 mL of saturated NaCl solution and 10 μL aqueous internal standard mixture containing 34.4 ng μL^{-1} 1-methylethylbutyrate and 33.4 ng μL^{-1} 5-hexanol were added, and then the vials were sealed. Vials were incubated at 22 °C for 5 min and then sonicated at 25 °C in an ultrasonic bath for 5 min prior to headspace analysis. Headspace vial temperature was maintained at −1 °C using a cooled sample tray until sampling.

Vial headspace was analyzed using an Agilent 6890N gas chromatograph coupled with a 5975B mass selective detector (Agilent Technologies, Palo Alto, CA) and an automated Gerstel multipurpose sampler (MPS) equipped with a dynamic headspace sampler (DHS). Headspace vial temperature was maintained at −1 °C using a cooled sample tray until sampling. At the beginning of the headspace sampling sequence, vials were vortexed at 1000 rpm during incubation at 30 °C for 10 min prior to sampling. To sample, analyte was collected by sweeping 220 mL of He at 20 mL min^{-1} through the headspace and then a 60 mm (length) × 6 mm (OD) glass tube (trap) containing 90 mg of Tenax TA (60/80 mesh) and 60 mg of Carbosieve 3 (60/80 mesh) (Supelco, St. Louis, MO) maintained at 30 °C. After loading, water was removed from the trap by sweeping the sorption bed with 400 mL of He at 40 mL min^{-1} while the trap was heated to 35 °C.

Traps were desorbed at 20 mL min^{-1} with the inlet set in the solvent purge mode and purge pressure adjusted to the inlet pressure. The desorption temperature program started at 30 °C for 0.2 min, increasing at 720 °C min^{-1} to 300 °C and then holding for 3 min. Desorbed analyte was collected on glass bead-filled liner maintained at −145 °C for the entire desorption period.

Analyte was introduced into the GC column (HP-5MS, Agilent) (30 m × 250 μm × 0.25 μm) by heating the liner to 150 at 16 °C s^{-1} and then to a final temperature of 300 at 12 °C s^{-1}, which was held for 3 min. The He carrier linear velocity was 40 cm s^{-1}. The injection split ratio was 1:5. The oven temperature was 30 °C for 0.5 min and then increased to 300 at 12 °C min^{-1}. The detector was operated in the EI mode with transfer line, source, and quadrupole temperatures maintained at 250, 150, and 230 °C, respectively. Mass spectra ranging from m/z 30 to 600 were recorded.

LC-MS Evaluation. Frozen peel powder (0.5 g) was weighed into 2 mL opaque, screw-top microcentrifuge tubes previously chilled in N_2 (l) to which ∼100 μL of 0.5 mm (diameter) soda lime glass beads (BioSpec Products, Inc., Bartlesville, OK) was added. Tubes were placed at room temperature, and 100 μL (79.8 ng μL^{-1}) of α-tocopherol acetate internal standard followed by 0.71 mL of 2:1 acetone/0.2 M HEPES, pH 7.7, was added, and the tubes were centrifuged at 2000*g* for 15 s . Then another 0.71 mL of acetone/HEPES was added, after which the tubes were shaken vigorously for 1 min using a Mini Beadbeater (BioSpec Products, Inc.) and then centrifuged at 16200*g* for 1 min. The supernatant was transferred to a 13 × 100 mm borosilicate test tube (stored in the dark and on ice) using a borosilicate pipet. The pellet was washed twice by adding 1 mL of acetone, bead beating the sample for 30 s, and then centrifuging the mixture as described above. The pellet was then washed with 0.75 mL of hexanes and the supernatant transferred to the test tube containing the compiled buffered acetone extract. The test tube was vortexed for 15 s and the hexanes phase transferred to a clean test tube after the phases separated. Another 0.75 mL of hexanes was added directly to the extract, vortexed, and allowed to separate while the tubes were held on ice before transferring the hexanes phase to the collection tube. This step was repeated once. The hexanes phase was dried under a stream of N_2 (g), the residue dissolved in 250 μL of acetone, and the sample filtered using a 0.45 μm PTFE syringe filter prior to analysis.

Samples were analyzed by injecting 10 μL into a series 1100 HPLC system (Agilent Technologies) controlled by Chemstation (B.02.01) and equipped with a Chromolith Performance RP-18e (4.6 × 100 mm) monolithic reverse-phase column (EMD Chemicals, Inc., Gibbstown, NJ), a G1315B diode array detector, and a G1946D single-quadrupole mass selective detector using an atmospheric pressure chemical ionization (APCI) source. Elution solvents used for a linear gradient were (A) 80:20 methanol/deionized water and (B) ethyl acetate. The column temperature and mobile phase flow rate were 20 °C and 1.0 mL min^{-1}, respectively. The mobile phase was composed entirely of solvent A for the initial 2 min after sample injection, followed by a linear gradient of solvent A plus B until the makeup reached 65% B at 21 min, and then remained entirely solvent B until 35 min. The eluate was first analyzed by the DAD and then the MSD. The DAD continuously monitored and recorded spectra (190−700 nm) for the entire analysis.

The APCI spray chamber conditions were as follows: drying gas (N_2) flow, 4 L min^{-1}; drying gas temperature, 350 °C; nebulizer pressure, 414 kPa; vaporizer temperature, 425 °C; and coronal discharge, 4 μA. The fragmentor and capillary potentials were 170 and 4000 V, respectively. The MSD was adjusted to monitor positive ions in the scanning mode, continuously monitoring and recording the entire mass spectra within a m/z 100−1200 range.

Data Acquisition, Deconvolution, and Peak Identification. User-defined libraries were generated with the aid of the automated mass spectral deconvolution and identification system (AMDIS, National Institute of Standards, Gaithersburg, MD) to deconvolute GC-MS and LC-MS results and identify distinct chromatographic components. For GC-MS data, retention indices (RI) were generated for each sequence by comparing the retention times of C5−C22 or C10−C40 hydrocarbons evaluated under the same conditions as the samples with the retention times of sample components measured using either the headspace analysis or trimethylsilyl(oxime) protocols, respectively. When possible, extracts from each protocol were analyzed using each instrumental method to find compounds that were detected using more than a single method. To further decrease the likelihood of redundant evaluation, authentic standards representing metabolites with wide-ranging physical properties were also evaluated using each extraction/analysis system. Measurements from only one analytical method were used for each metabolite.

Calibration tables for both GC-MS and LC-MS evaluations were compiled using Chemstation (G1701DA rev. E; Agilent, Palo Alto, CA) from which the Qedit macro was used to evaluate each compound and provide peak areas for components. Mass spectral comparison with

Table 1. EI and APCI Mass Spectra of Features Identified and Example Putative Sesquiterpenoid and Triterpenoid Metabolites for Comparison[a]

metabolite or mass spectral tag	evaluation method	principal mass spectral peaks [*m*/*z* (% total)]
(*E*,*E*) α-farnesene	GC-EIMS, APCIMS[b]	LC-*EI* 204 (<1), 189 (1.4), 161 (3.4), 147 (1.5), 123 (34), 119 (37), 107 (43), 93 (100), 79 (45), 69 (62), 55 (52); *APCI* 205 (100), 149 (10.2), 123 (6.5).
mst (1590, 159) "sequiterpenoid"	GC-EIMS	202 (14), 159 (86), 131 (37), 117 (44), 105 (62), 91 (86), 67 (78), 41 (100)
2,6,10-trimethyldodeca-2,7(*E*),9(*E*),11-tetraen-6-ol (CTol)	LC-APCIMS	203 (100), 147 (11), 123 (8.6)
mst (21.5, 205) "sesquiterpenoid"	LC-APCIMS	205 (100), 149 (27), 121 (28)
ursolic acid	LC-APCIMS	471 (3.0), 457 (4.0), 453 (5.7), 439 (100), 411 (21), 393 (17), 203 (7.9), 191 (12)
mst (4.47, 499) "triterpenoid"	LC-APCIMS	545 (2.8), 513 (60), 499 (93), 481 (100), 455 (99), 439 (84), 421 (92)
β-sitosterol	LC-APCIMS	411 (100), 397 (46)
mst (21.88, 397) "triterpenoid"	LC-APCIMS	397 (100), 411 (2.6)

[a] Putative triterpenoids are labeled using their mass spectral tag [mst; (RI or RT, target ion)] and the class of compounds they are most closely linked to by mass spectral comparison. Retention indices (RI) were calculated for GC-MS data. [b] This metabolite was detected using both methods. Only GC-MS data were used for the statistical model. The APCI mass spectrum serves as a reference for other sequiterpenoid mass spectra in this table.

spectra cataloged in NIST05 (National Institute of Standards) and mass spectral interpretation aided in tentative identification of many of the components. Compound identifications are based on comparison of sample compound spectra and RIs or retention times (LC-MS) with authentic standards. Authentic standards were purchased from Sigma-Aldrich-Fluka (St. Louis, MO) or TCI (Portland, OR). Details of α-farnesene and 2,6,10-trimethyldodeca-2,7(*E*),9(*E*),11-tetraen-6-ol (CTol) purification and mass spectral description of CTol were outlined previously (*35*).

Statistical Modeling and Analyses. Raw peak area data were corrected by comparison of phenyl β-D-glucopyranoside [trimethylsilyl(oxime) protocol], 1-methylethyl butanoate (headspace analysis protocol), and α-tocopherol acetate (LC-MS protocol) in each sample with that in an external standard and then by sample fresh weight. None of the compounds used as internal standards were detected in unspiked samples.

Metabolite data were analyzed using partial least-squares discriminant analysis (PLS-DA) (*36*). PLS-DA relates variations in a limited number of response variables (*Y*-variables) to the variations of a large number of predictor variables (*X*-variables). PLS-DA is a regression technique in which the original *X*-data are projected onto a small number of underlying latent variables (LV), which are concurrently used for regression of the *Y*-data in such a way that the first LVs are most relevant for predicting the *Y*-variables.

In this metabolic profiling study, the metabolites were considered to be predictor variables, whereas treatment factors (untreated, DPA-treated, or 1-MCP-treated), storage time (0−183 days), and scald index (1−4) were considered to be response variables. The treatments factors were introduced as three separate categorical variables (reading either 0 or 1), whereas storage time and scald index were included as continuous variables. Both *X*- and *Y*-data were mean centered and scaled to unit variance to give all variables an equal chance to influence the model.

Separate analyses were performed on either the full data set or only on the data from the first two storage months. Metabolite profiles for the initial samples taken at day 0 were assigned to all three treatments. PLS-DA was performed using The Unscrambler version 9.6 (Camo A/S, Trondheim, Norway).

RESULTS AND DISCUSSION

Analyses of peel metabolites using three analytical methods allowed for wide coverage of both primary and secondary metabolites. Although GC-MS evaluation of trimethylsilyl-(oxime) derivatives provides a broad-based evaluation of many metabolites (*33*, *37*), it may underestimate the impact of secondary metabolism on fruit metabolism (*38*). To improve our metabolomic estimation, additional analyses were employed to evaluate key areas of secondary metabolism associated with apple ripening, including volatile and isoprenoid metabolism.

Known and unknown metabolites, detected using the GC-MS headspace analysis and the LC-MS nonpolar analysis methods, were combined with compounds detected using the trimethylsilyl(oxime) method (*33*). Trimethylsilyl(oxime) derivatization and LC-MS analysis of the nonpolar extract revealed redundant detection of a few metabolites, including α-farnesene, β-sitosterol, ursolic acid, and other putative triterpenoids with similar mass spectral features (**Table 1**). With the exception of sesquiterpenes, compounds detected using headspace GC-MS evaluation were not detectable using any of the other methods. When redundancies were found, data acquired using the method with the greatest sensitivity was used for metabolomic modeling. Overall, overlap among methods was negligible due to physical differences among metabolites extracted using different analyses and the inherent selectivity of each of the instrumental methods.

Groups of known metabolites included compounds that have significant primary and secondary metabolic functions or that can influence fruit quality such as sugars, organic acids, aldehydes, alcohols, esters, amino acids, sugar acids, sugar alcohols, polyols, phosphorylated compounds, phenolics, vitamins, and multiple classes of isoprenoids. This paper focuses only on both known and putative isoprenoid metabolites contributing to the overall metabolomic evaluation, although all detected metabolites were included in models. A number of unknowns were tentatively classified as sesquiterpenes and triterpenes on the basis of their mass spectral similarity to authentic standards.

Unknown compounds classified as sesquiterpenoids had electron ionization or APCI mass spectra similar to those of α-farnesene or CTol standards. Putative triterpenoids have mass spectral features similar to those of authentic ursolic acid and β-sitosterol standards as well as previously published mass spectra of a variety of ursane and oleane triterpenoids found in apples (*39*−*43*). Ursolic acid has been widely reported in apple peel (*22*, *44*). Free, glycosylated, and/or acylated campesterol, β-sitosterol (*45*), and 7β-hydroxystigmast-4-en-3-one (*42*) have been identified in apple. A wide variety of hydroxylated and acylated oleane and ursane triterpenoid acids as well as ursanyl aldehyde and alcohols have been characterized in apples (*42*, *43*). Recently, cinnamoyl and *p*-coumaryl derivatives of ursolic and oleanic acid have been identified in apple peel (*46*).

Multivariate PLS-DA models linked metabolites to specific treatment factors (untreated, DPA-treated, or 1-MCP-treated), storage duration (0−183 days), and scald index (1−4). The full PLS-DA models were limited to 12 LVs explaining >95% of the observed *Y*-variance with the first 6 LVs already explaining >80%. The discussion focuses on the first 3 LVs.

The PLS-DA models reveal considerable divergence of apple peel metabolomes with increasing storage duration and in response to DPA and 1-MCP treatment. PLS-DA models containing observations for all treatments from 1 week to 2 months demonstrate that metabolomic divergence had occurred after 1

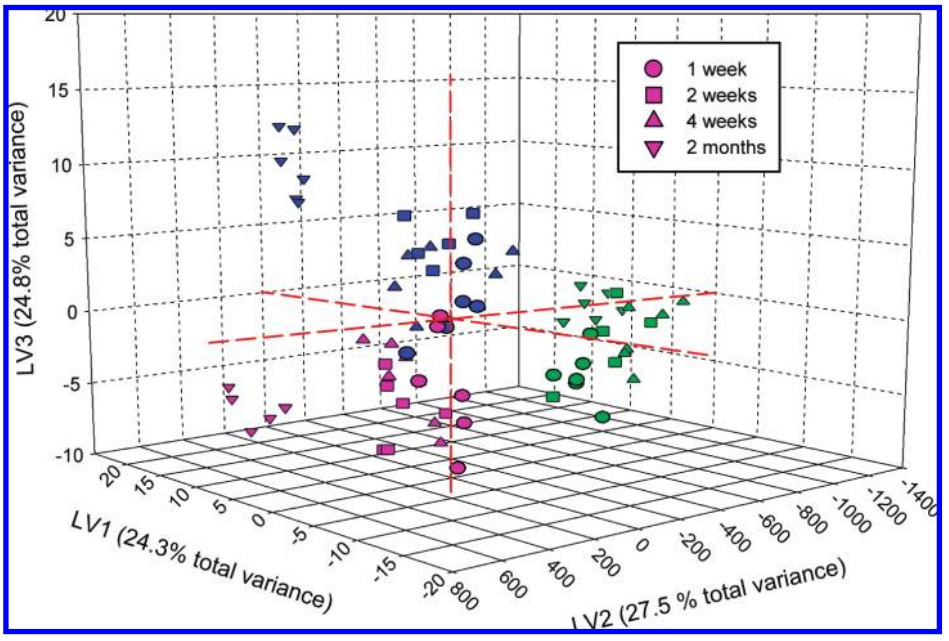

Figure 1. PLS-DA scores plot of the metabolic profile of untreated (pink), DPA-treated (blue), or 1-MCP-treated (green) 'Granny Smith' peel stored in air at 1 °C and sampled at 1, 2, and 4 weeks.

week of cold storage, especially for 1-MCP-treated fruit compared with control and DPA-treated fruit (**Figure 1**). However, the PLS-DA model using all observations (1 week−6 months) indicates that the rate of metabolomic divergence between the control and DPA-treated fruit increased between 1 week and 2 months (**Figure 2A**).

Whereas latent variables (LV) 1−2 highlight differences between the control and DPA-treated fruit, changes in the 1-MCP-treated fruit were more associated with LV3 (**Figure 2B**), which explains 46.3% of the 1-MCP treatment associated variation (**Table 2**). Transformation of control and DPA-treated fruit metabolomes along the LV1 axis is largely related to storage duration (74.4%), indicating similar ripeness of control and DPA-treated fruit with respect to storage duration. 1-MCP reduces the rate of apple fruit ripening during storage (*47*, *48*). The 1-MCP-treated fruit peel metabolome was not transformed to the same degree as the other two treatments on the LV1 axis, indicating it did not reach the same degree of ripeness during storage and supporting the link between LV1 and ripeness. The association between LV3 and the peel metabolome of 1-MCP-treated fruit with storage duration indicates 1-MCP-associated metabolism progresses differently with increasing storage duration from the other two treatments.

Scald symptoms appeared on control apples at 3 months and became more severe (**Figure 3A**), covering up to 95% of many fruits with widespread sunken necrotic spots by 6 months. The association between accelerated scald development and control fruit is likely the principal basis for separation of metabolomes of control and DPA-treated fruit, where only slight scald was detected at 6 months, on the LV2 axis. Both LV1 (45.7%) and LV2 (37.7%) explain a significant proportion of the scald-related variation in this model, indicating storage duration and DPA treatment nearly equally influence metabolite fluctuation and reflect how prolonged storage duration and oxidative stress are both required for scald development. LV2 scores for 1-MCP-treated fruit were similar to those of control fruit, which supports a relationship between LV2 and scald.

Delayed DPA treatment became completely ineffective after 2−4 weeks of storage, indicating that scald induction transpired

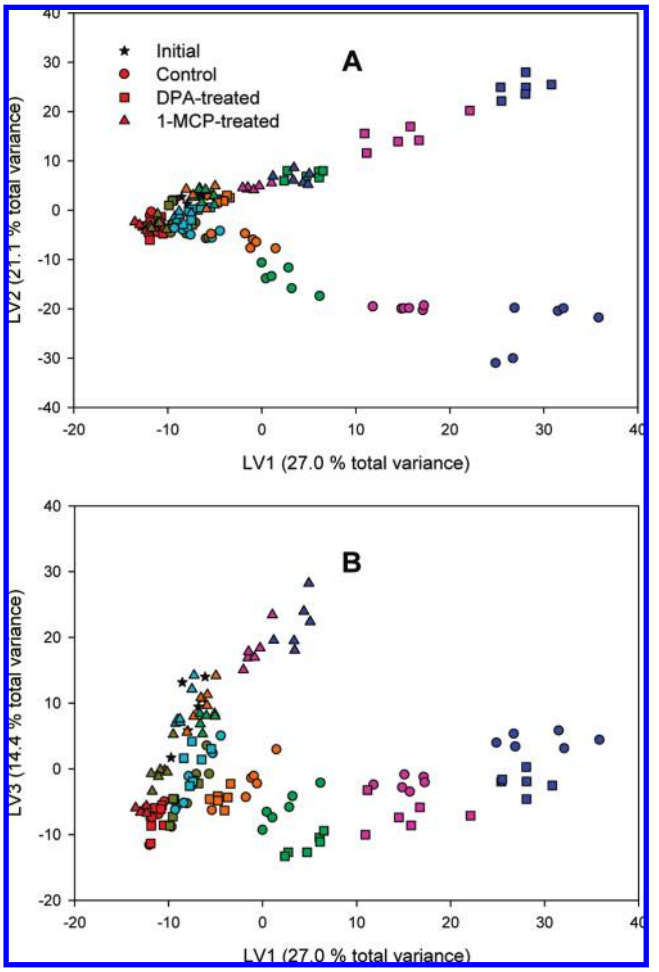

Figure 2. PLS-DA LV1−2 (**A**) and LV1−3 (**B**) scores plots of the metabolic profile of untreated, DPA-treated, or 1-MCP-treated 'Granny Smith' peel stored in air at 1 °C and sampled at 0 (black), 1 (red), 2 (brown), and 4 weeks (light blue) and 2 (orange), 3 (green), 4 (pink), and 6 months (blue).

Table 2. PLS-DA Total Explained Variance and Explained Variance for Latent Variables (LV) Broken down by Experimental Factor for both the 2 and 6 Month Models of 'Granny Smith' Apple Peel Metabolomes

	total variance	storage duration	untreated	DPA	1-MCP	scald
			Percent Variance Explained; 2 Month Model			
LV1	24.3	84.8	2.2	2.0	8.4	n/a
LV2	27.6	8.0	27.2	8.6	66.5	n/a
LV3	24.8	0.0	38.8	58.2	2.0	n/a
			Percent Variance Explained; 6 Month Model			
LV1	27.0	74.4	1.8	1.1	12.0	45.7
LV2	21.1	1.1	38.8	24.0	3.7	37.7
LV3	14.4	8.4	1.1	15.9	46.3	0.3

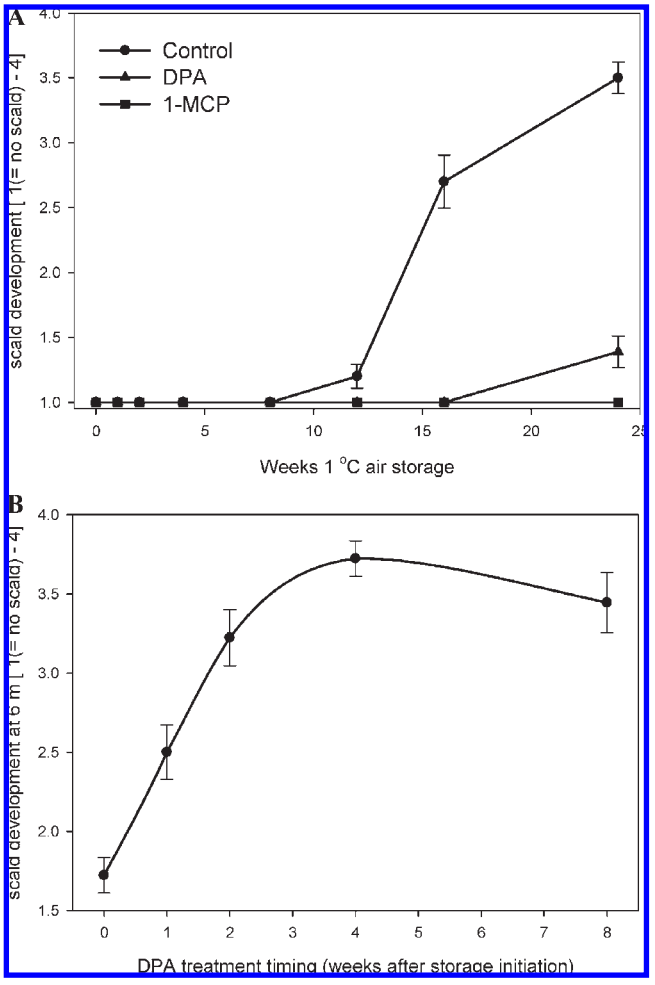

Figure 3. (**A**) Scald symptom development on untreated, DPA-treated, or 1-MCP-treated 'Granny Smith' apples stored at 1 °C. (**B**) Scald symptom development after 6 months of air storage at 1 °C on apples treated at 0, 1, 2, 4, or 8 weeks with 2 g L^{-1} DPA. Error bars represent SE (n = 18).

prior to 4 weeks of storage (**Figure 3B**). The end of this period coincides with the accelerated metabolomic divergence of control and DPA-treated fruit illustrated in the PLS-DA model. This indicates that extensive storage and treatment-related metabolomic changes may be arrested during scald induction or that subsequent events may trigger metabolic divergence between DPA-treated and control fruit.

Isoprenoid metabolites associated with untreated peel prior to or during scald development were revealed by overlaying the metabolite and experimental factor (Y-variables) loading plots. The combined plots show metabolite associations with specific experimental factors within the same plane as the treatments scores plots. The loading plot corresponding to **Figure 2A** reveals a close association between the α-farnesene oxidation products CTol, 6-methyl-5-hepten-2-one (MHO), 6-methyl-5-hepten-2-ol (MHOH), and scald (**Figure 4**). (*E*,*E*)-α-Farnesene, the principal farnesene isomer found in apples (*9*), (*Z*,*E*)-α-farnesene, and (*E*)-β-farnesene were more associated with DPA-treated fruit by 6 months. This confirms the relationship between farnesene oxidation product levels and scald development (*9*, *12*, *13*) while validating the statistical model showing a relationship between metabolome and scald. The model also highlights other areas of the metabolome that contributed to metabolic divergence among treatments for further investigation. In addition to the known isoprenoids, other putative sesquiterpenoids and triterpenoids were strongly associated with control fruit prior to or after scald development. The close association between putative ursane/oleane-like triterpenoids and scald is conceivably related to hydroxylation of ursolic or oleanic acid (*49*), a conversion that may be similar to oxidation of α-farnesene to various conjugated trienols (*50*).

Relationships between isoprenoid metabolism and control or DPA-treated fruit are revealed in the loading plot of the first three LVs from the 2 month model (**Figure 5**). This model indicates metabolism of certain isoprenoids in control fruit prior to the accelerated metabolic divergence depicted in the 6 month model. The 2 month model also links isoprenoid metabolism to the early segregation of the metabolomes from control and DPA-treated fruit that precede scald symptom development. In fact, increased levels of CTol, MHO, and MHOH were observed in control fruit after 2 weeks of storage (**Figure 6**). Similar trends in levels of these metabolites were detected in DPA-treated fruit, although levels were considerably reduced as indicated by the metabolite loading plots.

The results depict the widespread metabolomic changes associated with storage duration, antioxidant treatment, and ethylene insensitivity that precede and coincide with scald development. Prior work focusing on sequiterpenoid metabolism has demonstrated that α-farnesene oxidation precedes scald development (*10*, *11*), and a buildup of CTol and other conjugated trienol levels may actually have a direct role in provoking injury (*21*). The current results indicate that antioxidant-associated isoprenoid metabolism is altered beyond sesquiterpene metabolism, inviting additional scrutiny of this pathway and its relationship with storage-induced phenomena.

Multiple, putative triterpenoids are heavily involved in this system, suggesting that they may also have a role in scald development considering farnesyl diphosphate is a precursor of both sesquiterpenoids and triterpenoids in many biological systems (*51*). Triterpenoid biosynthesis proceeds via the mevalonic acid pathway in plants (*51*), although this has not been substantiated in apple fruit. Furthermore, treatment with lovastatin, an inhibitor of isoprenoid biosynthesis, reduces apple scald and α-farnesene biosynthesis (*52*) and, likewise, may conceivably reduce triterpenoid biosynthesis as it does in mammalian systems (*53*). As shown for conjugated trienol formation in apples, reduced synthesis of certain triterpenoids in DPA-treated fruit indicates oxidation may be involved in their presence. However, roles can only be substantiated with positive triterpenoid identification, demonstrating the presence of oxidized metabolites, coupled with analysis of metabolic cofluctuation within the detected portion of the isoprenoid pathway.

Untargeted, broad metabolomic analysis demonstrates differences provoked by DPA treatment were manifest in diverse pathways and indicates oxidation is an important component

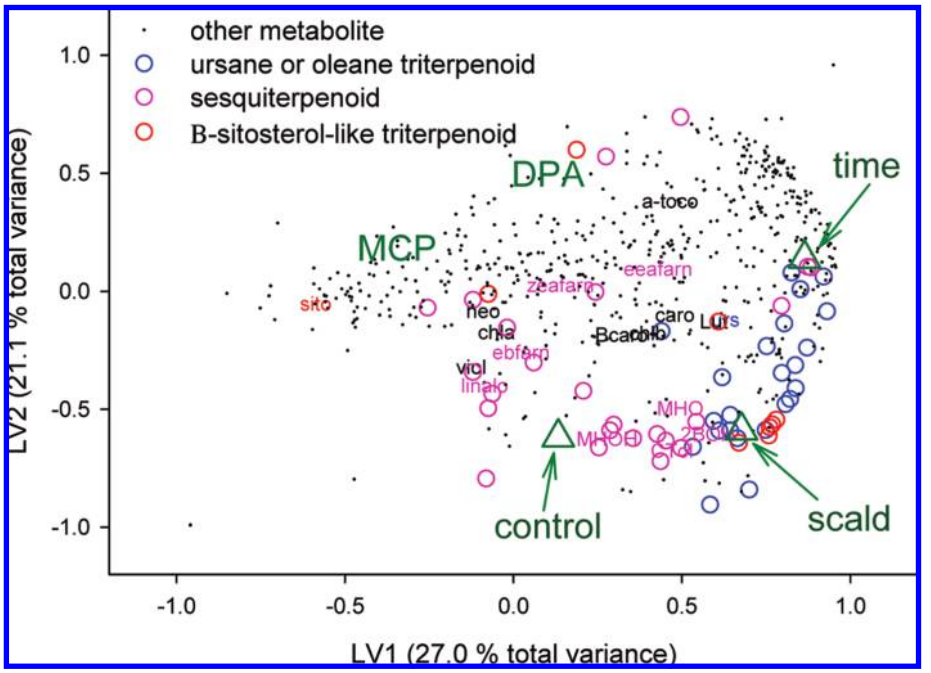

Figure 4. PLS-DA overlaid metabolite and *Y*-variable (experimental factor) loading plot including highlighted known and putative sesquiterpenoids and triterpenoids within the metabolic profile of untreated, DPA-treated, or 1-MCP-treated 'Granny Smith' peel stored in air at 1 °C and sampled at 1, 2, and 4 weeks and 2, 4, and 6 months.

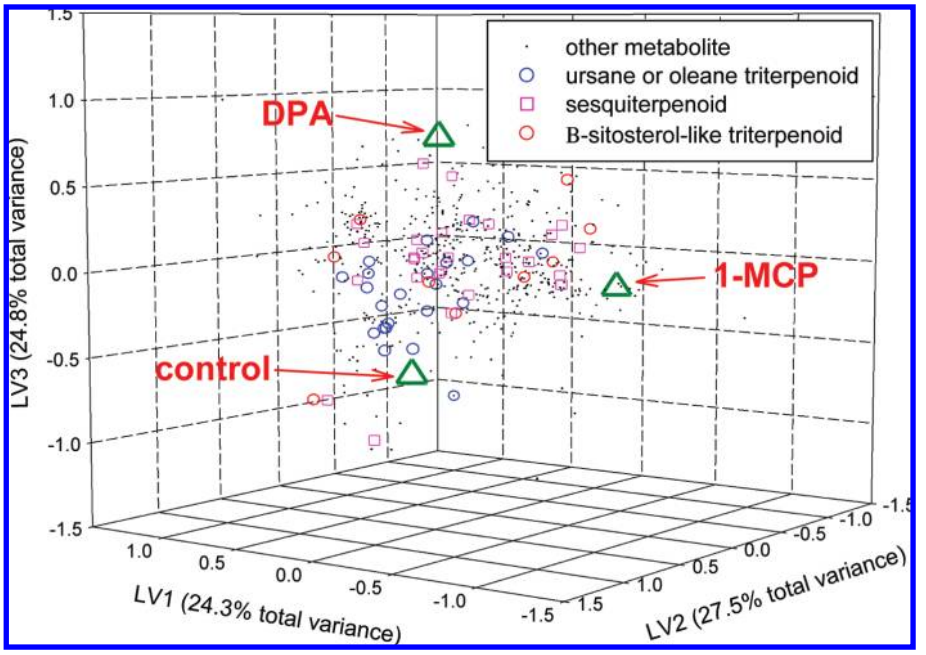

Figure 5. PLS-DA overlaid metabolite and *Y*-variable (experimental factor) loading plot including highlighted known and putative sesquiterpenoids and triterpenoids within the metabolic profile of untreated, DPA-treated, or 1-MCP-treated 'Granny Smith' peel stored in air at 1 °C and sampled at 1, 2, and 4 weeks.

of apple peel metabolism during storage ripening. Ripening and oxidative stress are often associated (*54*, *55*), although, interestingly, DPA has an immediate, yet only temporary, effect on apple ripening (*8*). The current results show little difference between metabolomes of control and DPA-treated fruit in relation to LV1, which is most representative of ripeness.

Chilling can provoke or enhance the apple ripening process (*56*, *57*) and is necessary to trigger ripening of certain pear cultivars (*58*). Likewise, chilling can enhance oxidative stress associated with low-temperature injury in many species (*59*) including tomato fruit, in which chilling also provokes changes in triterpenoid metabolism (*60*, *61*). In apple, chilling provokes increases in reactive oxygen species (ROS) and related enzyme activity that have been linked to scald development later in storage (*17*, *18*). Sequentially delayed 1-MCP and DPA treatment of 'Rome Beauty' and 'Cortland' apples becomes ineffective within the first month of storage (*20*), illustrating the importance of the first 2 months of storage in the scald induction process.

In the current study, sequentially delayed DPA treatment was used to define the length of the scald induction period.

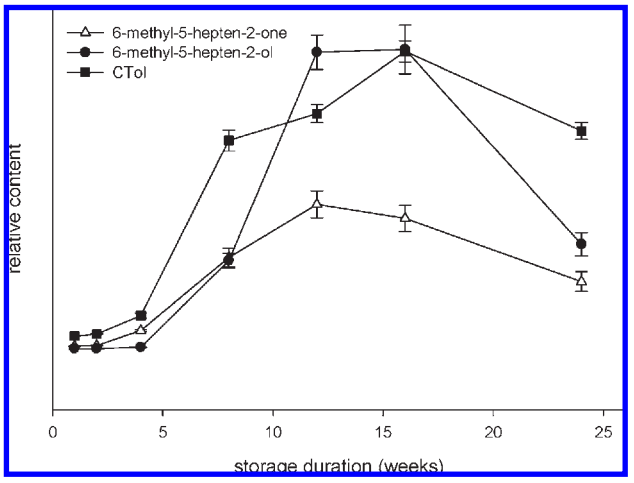

Figure 6. Fluctuation of three major products of farnesene metabolism in untreated 'Granny Smith' peel during air storage at 1 °C for 6 months. Error bars represent SE (n = 6).

In agreement with previous results, this event was complete within the first month of storage and was closely followed by accelerated divergence of the metabolomes of control and DPA-treated fruit between 1 and 2 months. This may reflect an incipient sequence of events whereby radical metabolomic change follows a gene induction or injury accumulation process or is just restrained by yet unknown mechanisms. Most prior evidence supports a gene induction period when increased enzyme activity associated with ROS metabolism transpires immediately following storage inception, yet well before symptom development occurs, as is the case with all of these events.

The temporal gap between scald induction, metabolomic divergence associated with widespread oxidation, and symptom development reported here influences current understanding of the impact oxidative stress may have on storage metabolism and superficial scald induction and development while providing some practical opportunities. As hypothesized, the scald inception and development period were characterized by metabolomic shifts in multiple pathways that may be exploited to develop storage management tools.

Clearly, more information regarding additional pathways coinciding with metabolite identification will render more information from the current model. Analyses focusing on correlative networks of metabolites are required to begin to understand the sequence of metabolic fluctuations related to different experimental factors. Finally, identification and localization of triterpenoids, which were a major component of the metabolomic change associated with oxidation, will be crucial to understanding the nature of changes within this undercharacterized class of peel metabolites.

ACKNOWLEDGMENT

We thank Dr. David Felicetti, David Buchanan, Bradley Wright, Laurel Mundy, and Yanina Perez Cayo for their assistance.

LITERATURE CITED

(1) Watkins, C. B.; Kupferman, E.; Rosenberger, D. A. Apple. In *The Commercial Storage of Fruits, Vegetables, And Florist and Nursery Stocks*; Gross, K., Ed.; USDA-ARS Handbook 66; U.S. GPO: Washington, DC, 2004.

(2) Watkins, C. B.; Bramlage, W. J.; Cregoe, B. A. Superficial scald of Granny Smith apples is expressed as a typical chilling injury. *J. Am. Soc. Hortic. Sci.* **1995**, *12*, 88–94.

(3) Bain, J. M. A. A histological study of the development of superficial scald in Granny Smith apples. *J. Hortic. Sci.* **1956**, *31*, 234–238.

(4) Brooks, C.; Cooley, J. S.; Fisher, D. F. Nature and control of apple scald. *J. Agric. Res.* **1919**, *18*, 211–220.

(5) Smith, W. H. Control of superficial scald in stored apples. *Nature* **1959**, *183*, 760.

(6) Smock, R. M. A comparison of treatments for control of the apple scald disease. *Proc. Am. Soc. Hortic. Sci.* **1957**, *69*, 91–100.

(7) Hardenburg, R. E.; Anderson, R. E. Postharvest chemical, hotwater, and packaging treatments to control apple scald. *Proc. Am. Soc. Hortic. Sci.* **1965**, *87*, 93–99.

(8) Whitaker, B. D. Oxidative stress and superficial scald of apple fruit. *HortScience* **2004**, *39*, 933–937.

(9) Huelin, F. E.; Murray, K. E. α-Farnesene in the natural coating of apples. *Nature* **1966**, *210*, 1260–1261.

(10) Huelin, F. E.; Coggiola, I. M. Superficial scald, a functional disorder of stored apples IV: Effect of variety, maturity, oiled wraps and diphenylamine on the concentration of α-farnesene in fruit. *J. Sci. Food Agric.* **1968**, *19*, 297–301.

(11) Whitaker, B. D.; Nock, J. F.; Watkins, C. B. Peel tissue α-farnesene and conjugated trienol concentrations during storage of 'White Angel' × 'Rome Beauty' apple selections susceptible and resistant to superficial scald. *Postharvest Biol. Technol.* **2000**, *20*, 231–241.

(12) Anet, E. F. L. J. Superficial scald, a functional disorder of stored apples VIII: volatile products from the autoxidation of α-farnesene. *J. Sci. Food Agric.* **1972**, *23*, 605–608.

(13) Mir, N.; Perez, R.; Beaudry, R. M. A poststorage burst of 6-methyl-5-hepten-2-one (MHO) may be related to superficial scald development in 'Cortland' apples. *J. Am. Soc. Hortic. Sci.* **1999**, *124*, 173–176.

(14) Huelin, F. E.; Coggiola, I. M. Superficial scald, a functional disorder of stored apples V: Oxidation of α-farnesene and its inhibition by diphenylamine. *J. Sci. Food Agric.* **1970**, *21*, 44–48.

(15) Gong, Y.; Tian, M. S. Inhibitory effect of diazocyclopentadiene on the development of superficial scald in Granny Smith apple. *Plant Growth Regul.* **1998**, *26*, 117–121.

(16) Fan, X.; Mattheis, J. P.; Blankenship, S. Development of apple superficial scald, soft scald, core flush, and greasiness is reduced by MCP. *J. Agric. Food Chem.* **1999**, *47*, 3063–3068.

(17) Fernández-Trujillo, J. P.; Nock, J. F.; Kupferman, E. M.; Brown, S. K.; Watkins, C. B. Peroxidase activity and superficial scald development in apple fruit. *J. Agric. Food Chem.* **2003**, *51*, 7182–7186.

(18) Kochar, S.; Watkins, C. B.; Conklin, P. L.; Brown, S. K. A quantitative and qualitative analysis of antioxidant enzymes in relation to susceptibility of apples to superficial scald. *J. Am. Soc. Hortic. Sci.* **2003**, *128*, 910–916.

(19) Shaham, Z.; Lers, A.; Lurie, S. Effect of heat or 1-methylcyclopropene on anti-oxidative enzyme activities and antioxidants in apples in relation to superficial scald development. *J. Am. Soc. Hortic. Sci.* **2003**, *128*, 761–766.

(20) Jung, S. K.; Watkins, C. B. Superficial scald control after delayed treatment of apple fruit with diphenylamine (DPA) and 1-methylcyclopropene (1-MCP). *Postharvest Biol. Technol.* **2008**, *50*, 45–52.

(21) Rowan, D. D.; Hunt, M. B.; Fielder, S.; Norris, J.; Sherburn, M. S. Conjugated triene oxidation products of α-farnesene induce symptoms of superficial scald on stored apples. *J. Agric. Food Chem.* **2001**, *49*, 2780–2787.

(22) Huelin, F. E. Superficial scald, a functional disorder of stored apples II: promoters and inhibitors. *J. Sci. Food Agric.* **1964**, *15*, 227–236.

(23) Meir, S.; Bramlage, W. J. Antioxidant activity in 'Cortland' apple peel and susceptibility to superficial scald after storage. *J. Am. Soc. Hortic. Sci.* **1988**, *113*, 412–418.

(24) Tsantili, E.; Gapper, N. E.; Arquiza, J.; Whitaker, B. D.; Watkins, C. B. Ethylene and α-farnesene metabolism in green and red skin of three apple cultivars in response to 1-methylcyclopropene (1-MCP) treatment. *J. Agric. Food Chem.* **2007**, *55*, 5267–5276.

(25) Rudell, D. R.; Mattheis, J. P. Superficial scald development and related metabolism is modified by postharvest light irradiation. *Postharvest Biol. Technol.* **2009**, *51*, 174–182.

(26) Goodacre, R.; Vaidyanathan, S.; Dunn, W. B.; Harrigan, G. G.; Kell, D. B. Metabolomics by numbers: acquiring and understanding global metabolite data. *Trends Biotechnol*. **2004**, *22*, 245–252.
(27) Fernie, A. R. The future of metabolic phytochemistry: larger numbers of metabolites, higher resolution, greater understanding. *Phytochemistry* **2007**, *68*, 2861–2880.
(28) Roessner-Tunali, U.; Hegemann, B.; Lytovchenko, A.; Carrari, F.; Bruedigam, C.; Granot, D.; Fernie, A. R. Metabolic profiling of transgenic tomato plants overexpressing hexokinase reveals that the influence of hexose phosphorylation diminishes during fruit development. *Plant Physiol*. **2003**, *133*, 84–99.
(29) Bino, R. J.; de Vos, C. H. R.; Lieberman, M.; Hall, R. D.; Bovy, A.; Jonker, H. H.; Tikunov, Y.; Lommen, A.; Moco, S.; Levin, I. The light-hyperresponsive high pigment-2(dg) mutation of tomato: alterations in the fruit metabolome. *New Phytol*. **2005**, *166*, 427–438.
(30) Mintz-Oron, S.; Mandel, T.; Rogachev, I.; Feldberg, L.; Lotan, O.; Yativ, M.; Wang, Z.; Jetter, R.; Venger, I.; Adato, A.; Aharoni, A. Gene expression and metabolism in tomato fruit surface tissues. *Plant Physiol*. **2008**, *147*, 823–851.
(31) Aharoni, A.; De Vos, C. H. R.; Verhoeven, H. A.; Maliepaard, C. A.; Kruppa, R.; Bino, R.; Goodenowe, D. B. Nontargeted metabolome analysis by use of Fourier transform ion cyclotron mass spectrometry. *OMICS: J. Integr. Biol*. **2002**, *6*, 217–234.
(32) Pedreschi, R.; Franck, C.; Lammertyn, J.; Erban, A.; Kopka, J.; Hertog, M.; Verlinden, B.; Nicolaï, B. Metabolic profiling of 'Conference' pears under low oxygen stress. *Postharvest Biol. Technol*. **2009**, *51*, 123–130.
(33) Rudell, D. R.; Mattheis, J. P.; Curry, E. A. Prestorage ultraviolet−white light irradiation alters apple peel metabolome. *J. Agric. Food Chem*. **2008**, *56*, 1138–1147.
(34) Rudell, D. R.; Mattheis, J. P.; Fellman, J. K. Influence of ethylene action, storage atmosphere, and storage duration on diphenylamine and diphenylamine derivative content of Granny Smith apple peel. *J. Agric. Food Chem*. **2006**, *54*, 2365–2371.
(35) Rudell, D. R.; Mattheis, J. P.; Fellman, J. K. Relationship of superficial scald development and α-farnesene oxidation to reactions of diphenylamine and diphenylamine derivatives in cv. Granny Smith apple peel. *J. Agric. Food Chem*. **2005**, *53*, 8382–8389.
(36) Pérez-Enciso, M.; Tenenhaus, M. Prediction of clinical outcome with microarray data: A partial least squares discriminant analysis (PLS-DA) approach. *Hum. Genet*. **2003**, *112*, 581–592.
(37) Roessner, U.; Wagner, C.; Kopka, J.; Trethewey, R. N.; Willmitzer, L. Simultaneous analysis of metabolites in potato tuber by gas chromatography−mass spectrometry. *Plant J*. **2000**, *23*, 131–142.
(38) Fernie, A. R.; Trethewey, R. N.; Krotzky, A. J.; Willmitzer, L. Innovation—metabolite profiling: from diagnostics to systems biology. *Nat. Rev. Mol. Cell Biol*. **2004**, *5*, 763–769.
(39) Siddiqui, S.; Hafeez, F.; Begum, S.; Siddiqui, B. Kaneric acid, a new triterpene from the leaves of *Nerium oleander*. *J. Nat. Prod*. **1986**, *49*, 1086–1090.
(40) Cheng, D.; Cao, X. Pomolic acid derivatives from the root of *Sanguisorba officinalis*. *Phytochemistry* **1992**, *31*, 1317–1320.
(41) Hota, R. K.; Bapuji, M. Triterpenoids from the resin of *Shorea robusta*. *Phytochemistry* **1994**, *35*, 1073–1074.
(42) Cefarelli, G.; D'Abrosca, B.; Fiorentino, A.; Izzo, A.; Mastellone, C.; Pacifico, S.; Pisocopo, V. Free-radical-scavenging and antioxidant activities of secondary metabololites from reddened cv. Annurca apple fruits. *J. Agric. Food. Chem*. **2006**, *54*, 803–809.
(43) D'Abrosca, B.; Fiorentino, A.; Monaco, P.; Oriano, P.; Pacifico, S. Annurcoic acid: a new antioxidant ursane triterpene from fruits of cv. Annurca apple. *Food Chem*. **2006**, *98*, 285–290.
(44) Sando, C. E. Constituents of the wax-like coating on the surface of the apple. *J. Biol. Chem*. **1923**, *56*, 457–468.
(45) Picchioni, G. A.; Watada, A. E.; Conway, W. S.; Whitaker, B. D.; Sams, C. E. Phospholipid, galactolipid, and steryl lipid composition of apple fruit cortical tissue following postharvest $CaCl_2$ infiltration. *Phytochemistry* **1995**, *39*, 763–769.
(46) He, X.; Liu, R. H. Triterpenoids isolated from apple peels have potent antiproliferative activity and may be partially responsible for apple's anticancer activity. *J. Agric. Food Chem*. **2007**, *55*, 4366–4370.
(47) Fan, X. T.; Blankenship, S. M.; Mattheis, J. P. 1-Methylcyclopropene inhibits apple ripening. *J. Am. Soc. Hortic. Sci*. **1999**, *124*, 690–695.
(48) Watkins, C. B.; Nock, J. F.; Whitaker, B. D. Responses of early, mid and late season apple cultivars to postharvest application of 1-methylcyclopropene (1-MCP) under air and controlled atmosphere storage conditions. *Postharvest Biol. Technol*. **2000**, *19*, 17–32.
(49) Majumder, P. L.; Chakraborty, M. Reinvestigation of the action of hydrogen peroxide on ursolic acid acetate. *Tetrahedron* **1979**, *35*, 2397–2403.
(50) Rowan, D. D.; Allen, J. M.; Fielder, S.; Spicer, J. A. Identification of conjugated triene oxidation products of α-farnesene in apple skin. *J. Agric. Food Chem*. **1995**, *43*, 2040–2045.
(51) Croteau, R.; Kutchan, T. M.; Lewis, N. G. Natural products (secondary metabolites). In *Biochemistry and Molecular Biology of Plants*; Buchanan, B. B., Gruissem, W., Jones, R. L., Eds.; American Society of Plant Physiologists: Rockville, MD, 2002; pp 1250−1318.
(52) Ju, Z.; Curry, E. A. Lovastatin inhibits α-farnesene synthesis without affecting ethylene production during fruit ripening in 'Golden Supreme' apples. *J. Am. Soc. Hortic. Sci*. **2000**, *125*, 105–110.
(53) Alberts, A. W.; Chen, J.; Kuron, G.; Hunt, V.; Huff, J.; Hoffman, C.; Rothrock, J.; Lopez, M.; Joshua, H.; Harris, E.; Patchett, A.; Monagan, R.; Currie, S.; Stapley, E.; Albers-Schonberg, G.; Hensens, O.; Hirshfield, J.; Hoogsteen, K.; Liesch, J.; Springer, J. Mevinolin: a highly potent competitive inhibitor of hydroxymethylglutaryl-coenzyme A reductase and a cholesterol-lowering agent. *Proc. Natl. Acad. Sci. U.S.A*. **1980**, *77*, 3957–3961.
(54) Brady, C. J. Fruit ripening. *Annu. Rev. Plant Physiol*. **1987**, *38*, 155–179.
(55) Masia, A. Superoxide dismutase and catalase activities in apple fruit during ripening and postharvest and with special reference to ethylene. *Physiol. Plant*. **1998**, *104*, 668–672.
(56) Knee, M.; Looney, N. E.; Hatfield, S. G. S.; Smith, S. M. Initiation of rapid ethylene synthesis by apple and pear fruits in relation to storage temperature. *J. Exp. Bot*. **1983**, *34*, 1207–1212.
(57) Jobling, J.; McGlasson, W. B.; Dilley, D. R. Induction of ethylene synthesizing competency in Granny Smith apples by exposure to low temperature in air. *Postharvest Biol. Technol*. **1991**, *1*, 111–118.
(58) Villalobos-Acuña, M.; Mitcham, E. J. Ripening of European pears: the chilling dilemma. *Postharvest Biol. Technol*. **2008**, *49*, 187–200.
(59) Lurie, S. Postharvest heat treatments. *Postharvest Biol. Technol*. **1998**, *14*, 257–269.
(60) Whitaker, B. D. Changes in lipids of tomato fruit stored at chilling and non-chilling temperatures. *Phytochemistry* **1991**, *30*, 757–761.
(61) McDonald, R. E.; McCollum, T. G.; Baldwin, E. A. Prestorage heat treatments influence free sterols and flavor volatiles of tomatoes stored at chilling temperature. *J. Am. Soc. Hortic. Sci*. **1996**, *121*, 531–536.

Received May 11, 2009. Revised manuscript received July 28, 2009. Accepted August 03, 2009. We thank the Washington Tree Fruit Research Commission for funding this research.